

Supporting Information

Advancing Recyclable Thermosets through C=C/C=N Dynamic Covalent Metathesis Chemistry

Jie Zheng,^a Hongzhi Feng,^{a,b} Xinglong Zhang,^c Jianwei Zheng,^c Jeffrey Kang Wai Ng,^a Sheng Wang,^{a,*} Nikos Hadjichristidis,^{d,*} Zibiao Li^{a,e,f,*}

^a Institute of Sustainability for Chemicals, Energy and Environment (ISCE²), Agency for Science, Technology and Research (A^{*}STAR), 1 Pesek Road, Jurong Island, Singapore 627833, Republic of Singapore.

^b Key Laboratory of Bio-Based Polymeric Materials Technology and Application of Zhejiang Province, Laboratory of Polymers and Composites, Ningbo Institute of Materials Technology and Engineering, Chinese Academy of Sciences, Ningbo 315201, People's Republic of China

^c Institute of High Performance Computing (IHPC), Agency for Science, Technology, and Research (A^{*}STAR), Singapore 138632, Republic of Singapore.

^d Polymer Synthesis Laboratory, Chemistry Program, Physical Sciences and Engineering Division, KAUST Catalysis Center, King Abdullah University of Science and Technology (KAUST), Thuwal 23955, Saudi Arabia.

^e Institute of Materials Research and Engineering, Agency for Science, Technology, and Research (A^{*}STAR), 2 Fusionopolis Way, Innovis #08-03, Singapore 138634, Republic of Singapore.

^f Department of Materials Science and Engineering, National University of Singapore, 9 Engineering Drive 1, Singapore 117576, Republic of Singapore.

Correspondence to: wang_sheng@isce2.a-star.edu.sg;
nikolaos.hadjichristidis@kaust.edu.sa; lizb@imre.a-star.edu.sg.

8. DFT calculation

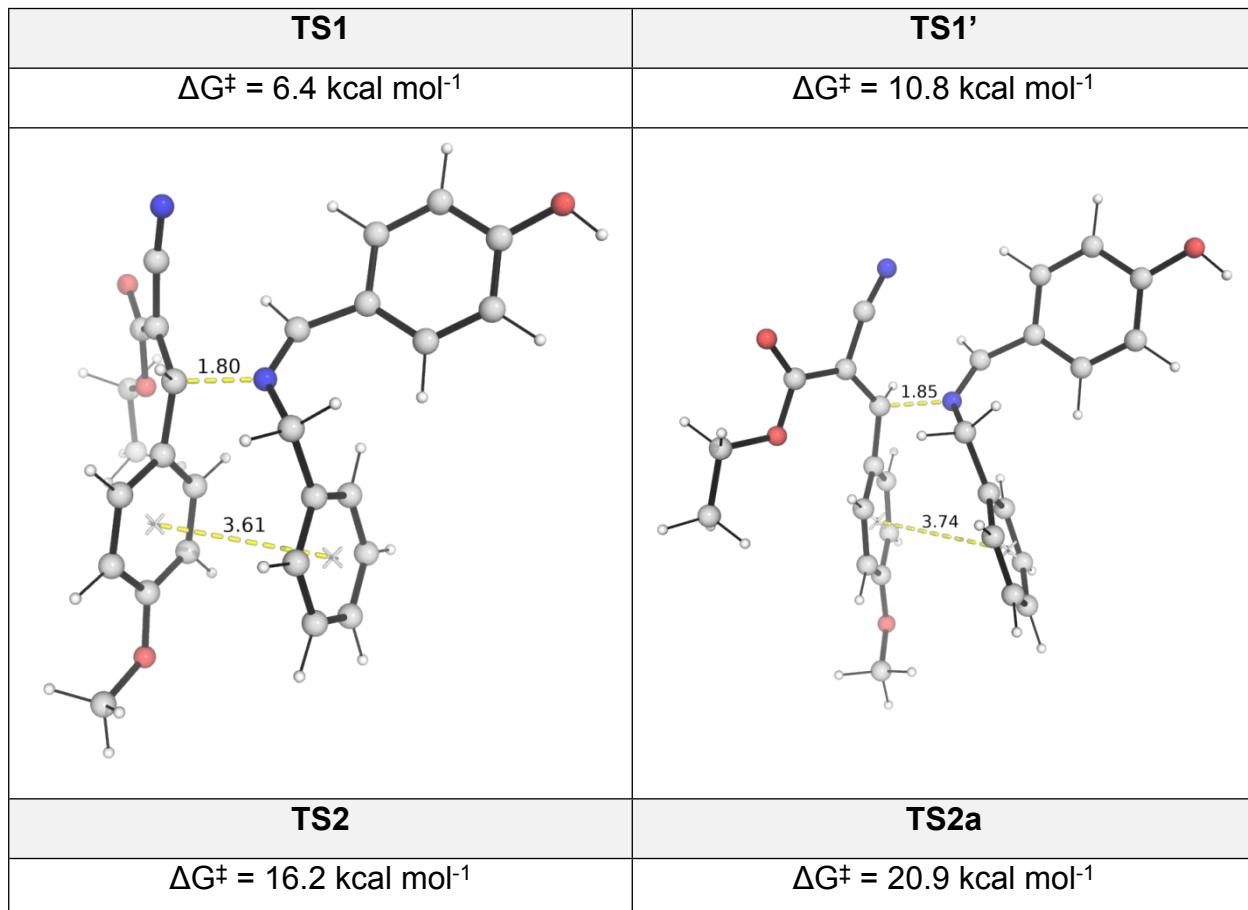
8.1 Computational Methods

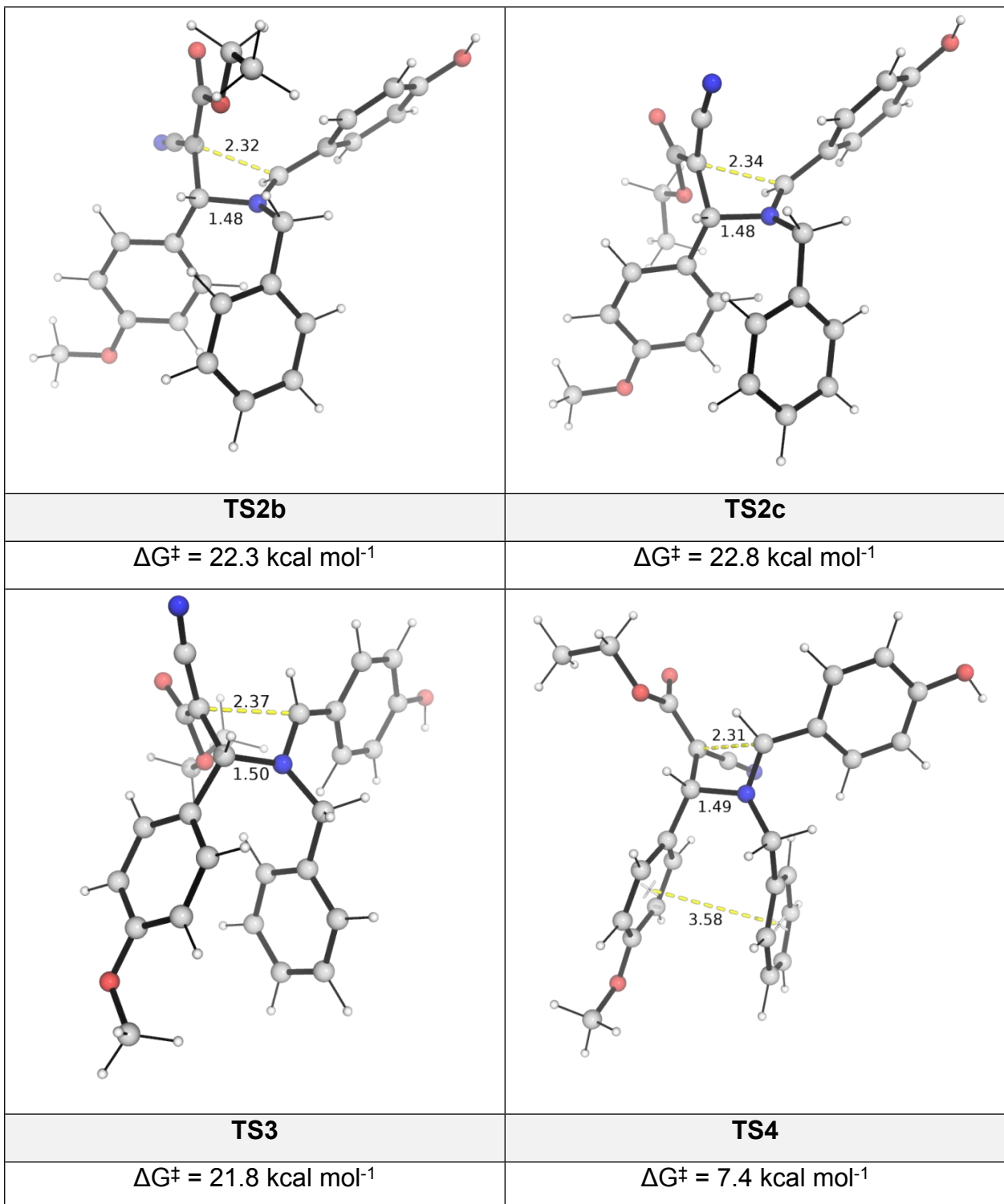
The global hybrid DFT functional M06-2X³ was employed with the Karlsruhe-family double- ζ valence def2-SVP^{4,5} basis set for all atoms to model the catalytic mechanism of the present transformation. For the M06-2X/def-SVP gas phase optimized structures, single point (SP) corrections were performed using M06-2X functional and def2-TZVP^{4,5} basis set for all atoms to improve upon the accuracy of the calculated energy. For each of these SP calculations, the implicit SMD continuum solvation model⁶ for dimethyl sulfoxide (DMSO) solvent was used to account for the effect of solvent on the potential energy surface (PES). All these calculations were performed with *Gaussian 16* rev. B.01 software.⁷

Gibbs energies were evaluated at room temperature (25 °C), using Grimme's scheme of quasi-RRHO treatment of vibrational entropies⁸, using the GoodVibes code⁹. Vibrational entropies of frequencies below 100 cm⁻¹ were obtained according to a free rotor description, using a smooth damping function to interpolate between the two limiting descriptions. The free energies reported in Gaussian from gas-phase optimization were further corrected using standard concentration of 1 mol/L,¹⁰⁻¹² which were used in solvation calculations, instead of the gas-phase 1atm used by default in *Gaussian* program.

8.2 DFT optimized structures

Geometries of all optimized structures (in xyz format with their associated energy in Hartrees) are included in a separate folder named DFT structures and uploaded to <https://zenodo.org/uploads/11280484> (DOI: 10.5281/zenodo.11280484).





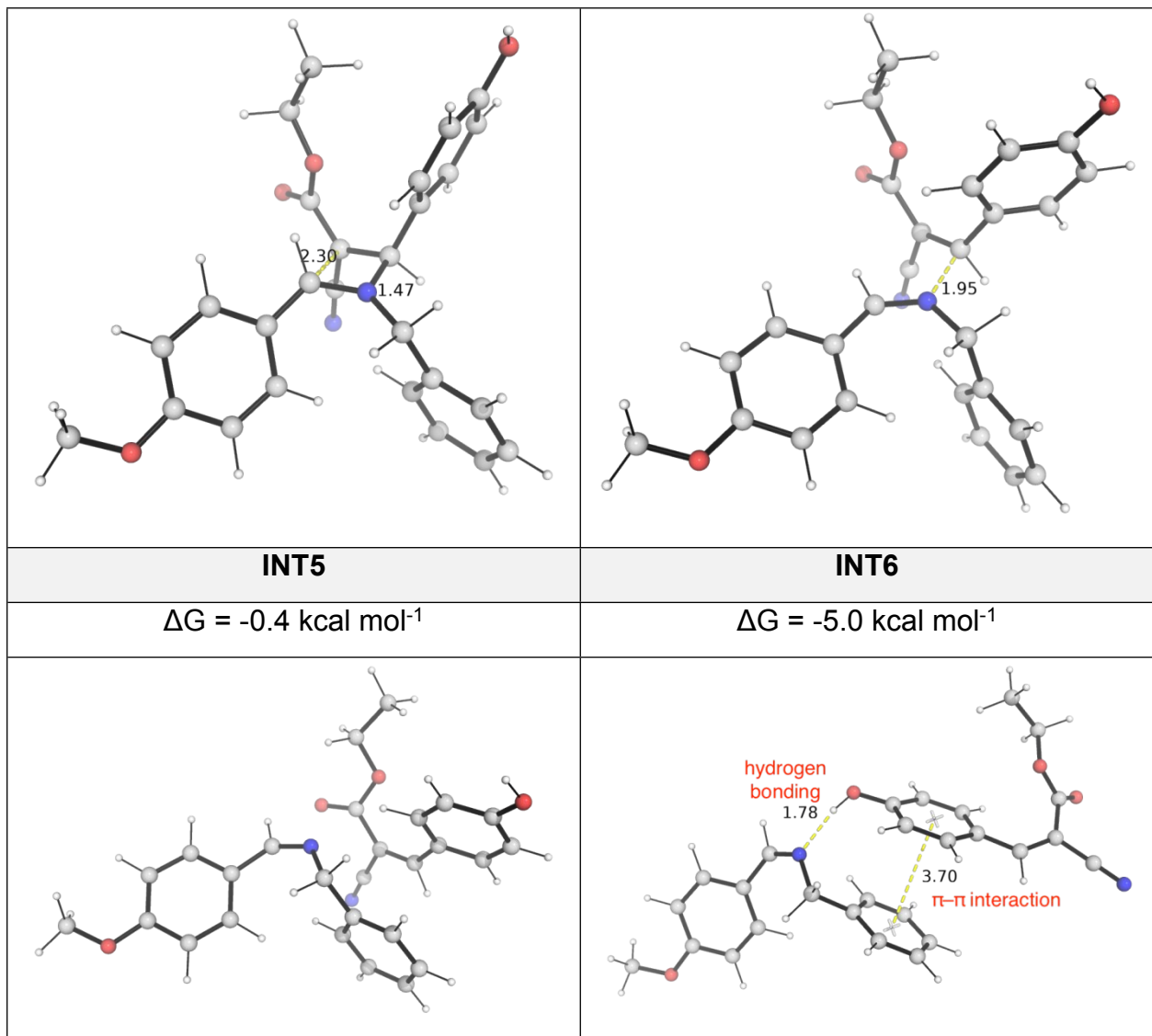


Figure S16. DFT optimized transition state structures and product complexes with key bond distances given in Å. **INT5** is the product complex resulting from **TS4**, and **INT6** is the product complex that is stabilized by π - π interaction and hydrogen bonding between phenol OH group and imine N atom.

8.3 Determination of selectivity ratio using simple transition state theory

The Eyring equation

$$k = \frac{k_B T}{h} e^{-\Delta G^\ddagger / RT}$$

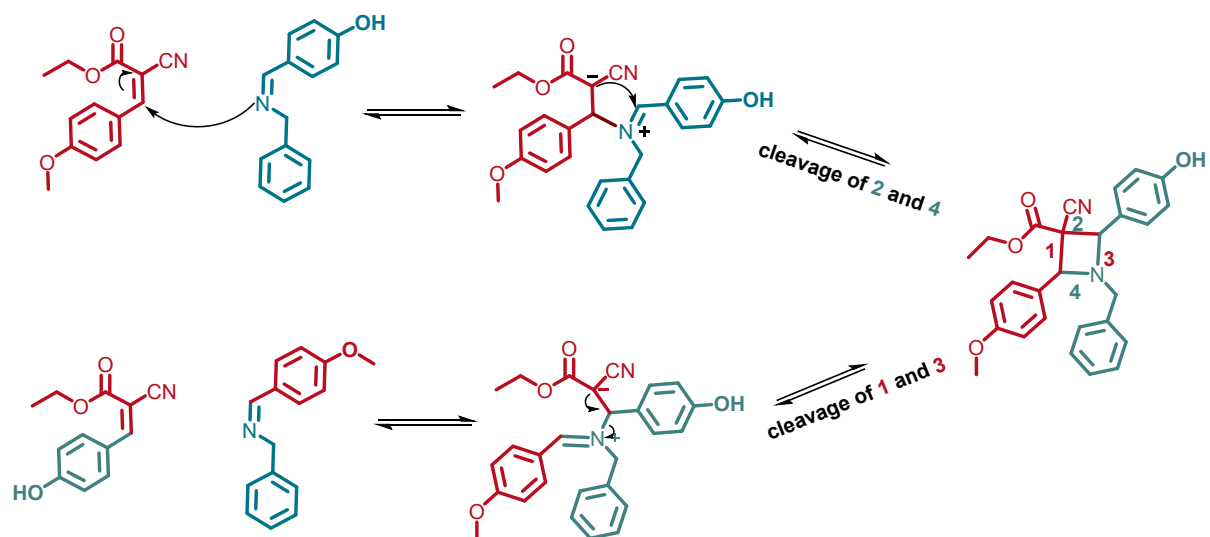
gives the rate constant under simple transition state theory (TST) assumptions.

Under kinetic control, as we compare the barrier heights difference between competing transition states, the ratio of the rates between two pathways is given by:

$$\frac{k_A}{k_B} = \frac{e^{-\Delta G_A^\ddagger / RT}}{e^{-\Delta G_B^\ddagger / RT}} = e^{-\Delta \Delta G^\ddagger / RT}$$

where k_X is the rate constant of pathway X (X=A or B); ΔG_X^\ddagger is the activation barrier for pathway X; and $\Delta \Delta G^\ddagger$ is the difference in the barrier heights; and R is the gas constant, T the temperature. Note that the Eyring Equation pre-exponential factor cancels when comparing the ratio of the rate constants. Thus, using the calculated $\Delta \Delta G^\ddagger$ value (difference of barrier heights between competing TSs) at the reaction temperature (e.g., 25°C = 298.15K), we are able to obtain the ratio of competing rates.

11. Proposed Mechanism



Scheme S5. Proposed Mechanism for the C=C/C=N exchange reaction in current system.

Table S5. Absolute values (in Hartrees) for SCF energy, zero-point vibrational energy (ZPE), enthalpy and quasi-harmonic Gibbs free energy (at 25°C/298.15 K) for optimized structures are given below. Single point corrections in SMD DMSO using M06-2X/def2-TZVP level of theory are also included.

Structur e	E/au	ZPE/au	H/au	T.S/au	qh-G/au	SP	
						SMD(DMSO)-	M06-2X/def2-
						TZVP	
INT1	-1453.206739	0.479231	-1452.6953	0.095626	-1452.782669	-1454.867958	
TS1	-1453.18657	0.480134	-1452.6755	0.091391	-1452.759837	-1454.860409	
INT2	-1453.187148	0.481158	-1452.6747	0.092654	-1452.759898	-1454.865265	
TS2a	-1453.165743	0.479872	-1452.6549	0.092394	-1452.739556	-1454.836732	
TS2	-1453.169756	0.480115	-1452.6589	0.091534	-1452.742991	-1454.844819	
INT3	-1453.218819	0.481933	-1452.706	0.091293	-1452.790215	-1454.876625	
TS2b	-1453.166441	0.480594	-1452.6556	0.088423	-1452.737938	-1454.836837	
TS2c	-1453.169755	0.480963	-1452.6584	0.089216	-1452.74142	-1454.835832	
TS3	-1453.167173	0.480212	-1452.6561	0.091287	-1452.740279	-1454.835999	
INT4	-1453.193145	0.481565	-1452.6802	0.09363	-1452.765713	-1454.87215	
TS4	-1453.186831	0.479338	-1452.6761	0.095148	-1452.762297	-1454.856644	
INT5	-1453.208289	0.479684	-1452.6964	0.096175	-1452.783959	-1454.868803	
INT6	-1453.212148	0.479403	-1452.7007	0.097267	-1452.788597	-1454.875463	
TS1'	-1453.182581	0.479873	-1452.6716	0.092987	-1452.756724	-1454.85192	

18. References

- 1 R. Gu, K. Flidrova and J. M. Lehn, Dynamic Covalent Metathesis in the C=C/C=N Exchange between Knoevenagel Compounds and Imines, *J. Am. Chem. Soc.*, 2018, **140**, 5560–5568.
- 2 Y. Nishimura, J. Chung, H. Muradyan and Z. Guan, Silyl Ether as a Robust and Thermally Stable Dynamic Covalent Motif for Malleable Polymer Design, *J. Am. Chem. Soc.*, 2017, **139**, 14881–14884.
- 3 Y. Zhao and D. G. Truhlar, The M06 suite of density functionals for main group thermochemistry, thermochemical kinetics, noncovalent interactions, excited states, and transition elements: two new functionals and systematic testing of four M06-class functionals and 12 other function, *Theor. Chem. Acc.*, 2008, **120**, 215–241.
- 4 F. Weigend and R. Ahlrichs, Balanced basis sets of split valence, triple zeta valence and quadruple zeta valence quality for H to Rn: Design and assessment of accuracy, *Phys. Chem. Chem. Phys.*, 2005, **7**, 3297–3305.
- 5 F. Weigend, Accurate Coulomb-fitting basis sets for H to Rn, *Phys. Chem. Chem. Phys.*, 2006, **8**, 1057–1065.
- 6 A. V. Marenich, C. J. Cramer and D. G. Truhlar, Universal solvation model based on solute electron density and on a continuum model of the solvent defined by the bulk dielectric constant and atomic surface tensions, *J. Phys. Chem. B*, 2009, **113**, 6378–6396.
- 7 M. J. . Frisch, G. W. . Trucks, H. B. . Schlegel, G. E. . Scuseria, M. A. . Robb, J. R. . Cheeseman, G. . Scalmani, V. . Barone, G. A. . Petersson, H. . Nakatsuji, X. . Li, M. . Caricato, A. V. . Marenich, J. . Bloino, B. G. . Janesko, R. . Gomperts, B. . Mennucci and D. J. Hratch, 2016.
- 8 S. Grimme, Supramolecular binding thermodynamics by dispersion-corrected density functional theory, *Chem.: Eur. J.*, 2012, **18**, 9955–9964.
- 9 G. Luchini, J. V. Alegre-Requena, I. Funes-Ardoiz, R. S. Paton and R. Pollice, GoodVibes: automated thermochemistry for heterogeneous computational chemistry data, 2020, **9**, 291.
- 10 V. S. Bryantsev, M. S. Diallo, W. A. Goddard III and W. A. Goddard, Calculation of Solvation Free Energies of Charged Solutes Using Mixed Cluster/Continuum Models, *J. Phys. Chem. B*, 2008, **112**, 9709–9719.
- 11 B. T. Boyle, J. N. Levy, L. de Lescure, R. S. Paton and A. McNally, Halogenation of the 3-position of pyridines through Zincke imine intermediates, *Science*, 2022, **378**, 773–779.
- 12 A. Darù, X. Hu and J. N. Harvey, Iron-Catalyzed Reductive Coupling of Alkyl Iodides with Alkynes to Yield cis-Olefins: Mechanistic Insights from Computation, *ACS Omega*, 2020, **5**, 1586–1594.

Full reference Gaussian 16:

Gaussian 16, Revision B.01, Frisch, M. J.; Trucks, G. W.; Schlegel, H. B.; Scuseria, G. E.; Robb, M. A.; Cheeseman, J. R.; Scalmani, G.; Barone, V.; Mennucci, B.; Petersson, G. A.; Nakatsuji, H.; Caricato, M.; Li, X.; Hratchian, H. P.; Izmaylov, A. F.; Bloino, J.; Zheng, G.; Sonnenberg, J. L.; Hada, M.; Ehara, M.; Toyota, K.; Fukuda, R.; Hasegawa, J.; Ishida, M.; Nakajima, T.; Honda, Y.; Kitao, O.; Nakai, H.; Vreven, T.; Montgomery Jr., J. A.; Peralta, J. E.; Ogliaro, F.; Bearpark, M.; Heyd, J. J.; Brothers, E.; Kudin, K. N.; Staroverov, V. N.; Kobayashi, R.; Normand, J.; Raghavachari, K.; Rendell, A.; Burant, J. C.; Iyengar, S. S.; Tomasi, J.; Cossi, M.; Rega, N.; Millam, J. M.; Klene, M.; Knox, J. E.; Cross, J. B.; Bakken, V.; Adamo, C.; Jaramillo, J.; Gomperts, R.; Stratmann, R. E.; Yazyev, O.; Austin, A. J.; Cammi, R.; Pomelli, C.; Ochterski, J. W.; Martin, R. L.; Morokuma, K.; Zakrzewski, V. G.; Voth, G. A.; Salvador, P.; Dannenberg, J. J.; Dapprich, S.; Daniels, A. D.; Farkas, Ö.; Foresman, J. B.; Ortiz, J. V; Cioslowski, J.; Fox, D. J. Gaussian, Inc., Wallingford CT, 2016.